Available online at www.sciencedirect.com
ScienceDirect
Trans. Nonferrous Met. Soc. China 23(2013) 1382−1389
Transactions of Nonferrous Metals Society of China
www.tnmsc.cn

Influence of nano-CeO_2 on coating structure and properties of electrodeposited Al/α-PbO_2/β-PbO_2

Zhen CHEN[1], Qiang YU[1], Deng-hui LIAO[2], Zhong-cheng GUO[2], Jian WU[2]

1. Faculty of Science, Kunming University of Science and Technology, Kunming 650093, China;
2. Faculty of Metallurgy and Energy Engineering, Kunming University of Science and Technology, Kunming 650093, China

Received 6 April 2012; accepted 10 September 2012

Abstract: Al/α-PbO_2/β-PbO_2 composite electrodes doped with rare earth oxide (CeO_2) were prepared by anodic oxidation method investigate the influence of nano-CeO_2 dopants on the properties of Al/α-PbO_2/β-PbO_2−CeO_2 electrodes and the impact of α-PbO_2 as the intermediate layer. The results show that using α-PbO_2 as the intermediate layer will benefit the crystallization of β-PbO_2 and β-PbO_2 is more suitable as the surface layer than α-PbO_2. CeO_2 dopants change the crystallite size and crystal structure, enhance the catalytic activity, and even change the deposition mechanism of PbO_2. The doping of CeO_2 in the PbO_2 electrodes can enhance the electro-catalytic activity, which is helpful for oxygen evolution, and therefore reduce the cell voltage.
Key words: rare earth; CeO_2; composite electrode material; α-PbO_2; β-PbO_2; cell voltage; inert anode

1 Introduction

Studies on inert anode materials used in zinc-plating industry have mostly focused on conventional anode materials, such as lead-based alloys, dimensionally stable anode, Au, Pt and glassy carbon [1−3]. However, the disadvantages of conventional anode materials including high cell voltage, poisonousness, low mechanical strength, inefficient conductivity and impurity product caused by anode re-dissolve have always perplexed us [4,5]. Therefore, further researches have been undertaken to discover more efficient electrode materials and metal oxide-film electrodes, such as PbO_2, SnO_2 and RuO_2 [6−10].

Lead dioxide (PbO_2) electrode has been extensively used in electrochemical industry and regarded as an excellent metal oxide electrode because of its low price compared with noble metals, good chemical stability, and high catalytic activity for oxygen evolution. The application of PbO_2 electrode is largely dependent upon its structure, morphology, and phase composition. In order to further improve the electrochemical properties of PbO_2 toward various applications, incorporating some ions or particles such as rare earth into the film of lead oxide was investigated.

It is well known that PbO_2 has two different crystallographic forms: orthorhombic and tetragonal (α and β). α-PbO_2 is obtained from alkaline solution and β-PbO_2 from acid solution [11]. α-PbO_2 has a better contact between particles, and a more compact structure than β-PbO_2. Unfortunately, more compact structure leads to bad conductivity compared with β-PbO_2 [12]. Different electro-catalytic activities of α and β forms of PbO_2 were observed in other studies. It was also observed that the structure of crystallization of PbO_2 films influenced the electro-catalytic properties of the material [13−19].

A new type of PbO_2 anode was widely used in electrolysis [20]. This electrode is made up of four layers: a metal base, a conductive layer (protecting the substrate from passivation), α-PbO_2 as the intermediate layer, and β-PbO_2 as surface layer. Aluminum is relatively cheap and has a good conductivity. The electrode material by electrodepositing lead dioxide on Al substrate has huge market prospects. Rare earth oxides, as powerful oxidants, can easily catalyze the oxidation of organics. It was reported that [21−24] metal

Foundation item: Project (50964008) supported by the National Natural Science Foundation of China; Project (2010287) supported by Analysis and Testing Foundation of Kunming University of Science and Technology, China
Corresponding author: Qiang YU; Tel: +86-13708460246; E-mail: yuqiang0015@163.com
DOI: 10.1016/S1003-6326(13)62607-2

oxides have been successfully doped into PbO_2 electrodes by anodic codeposition. However, few researches on the doping of rare earth oxide into PbO_2 electrodes have been reported.

In this work, α-PbO_2 was chosen as intermediate layer, and β-PbO_2 as the surface layer. Ce(IV) was introduced as a doping agent into PbO_2 electrode for its superior properties [25] were successfully doped by the anodic codeposition method. It changes the crystallite size and enhances the catalytic activity in the oxidation of the material. Scanning electron microscopy (SEM), X-ray diffraction (XRD) and energy-dispersive spectroscopy (EDS) were used to examine the changes in the coating.

2 Experimental

2.1 Preparation of coatings

After a series of pretreatments: sand blasting→ degreasing (40 g/L Na_3PO_4, 10 g/L Na_4SiO_4, 3 min)→ chemically etching (10 mL/L HF, 50 mL/L HNO_3, 90 s) → coating by a conductive layer, 1060# Al was used as an anode and machined to dimensions of 40 mm×10 mm×1 mm. Pure lead was used as a cathode. The electrodeposition of α-PbO_2 was conducted in an alkaline bath, while that of β-PbO_2 was conducted in an aqueous bath. The plating conditions are listed in Table 1 and Table 2, respectively. Two types of anodes were made: one was Al/conductive layer/β-PbO_2 (No. 1), and the other was Al/conductive layer/α-PbO_2/β-PbO_2 (No. 2). The difference between them was the intermediate layer α-PbO_2. CeO_2 was introduced as a doping agent into the aqueous β-PbO_2 electrolyte. By the anodic codeposition method, CeO_2 was successfully doped into No. 2 electrode.

2.2 Measuring instruments

Micrographs of the coating surface were obtained by scanning electron microscopy (ESEM, FEI, Quanta200). The structures of the films were analyzed by X-ray diffraction (XRD) with Co K_α radiation in a standard X-ray diffract meter (Rigaku D/max−1200X). The element contents were tested by energy-dispersive spectroscopy (EDAX-Phoenix). The over-potential was tested in 1.3 mol/L $ZnSO_4$+1 mol/L H_2SO_4 (pH=4.5) using polarization curves at a scanning rate of 50 mV/s. (CHI660D, Chenhua, China). During the measurement, a three-electrode system was used. The working electrode was the composite coating (1 cm×1 cm). The reference electrode was saturated calomel electrode (SCE) used directly in contact with the working solution. The counter electrode was platinum (1 cm×1 cm).The measurement was conducted at room temperature.

3 Results and discussion

3.1 Choice of intermediate layer

In this work, α-PbO_2 was obtained at a constant current density of 20 mA/cm^2 for 30 min in the solution containing 180 g/L NaOH saturated with PbO(s), and was used as the intermediate layer. A typical XRD pattern of α-PbO_2 deposited on Al/conductive layer is shown in Fig. 1. The surface morphology of α-PbO_2 coating is shown in Fig. 2. The XRD pattern indicates the presence of α-PbO_2. The characteristic peaks are α-PbO_2 (scrutinyite), and β-PbO_2 (plattnerite) is not observed. The grain of α-PbO_2 looks like rod or fiber. Numerous crystal edges and a few pores are found in such coating. However, these defects are proved to be helpful for the deposition of β-PbO_2 in further study.

The XRD patterns of two types of β-PbO_2 coatings (No. 1 and 2) shown in Fig. 3 all accord with the PDF#41—1492, which is plattnerite (β-PbO_2). No. 1 was prepared directly on the Al conductive layer, while

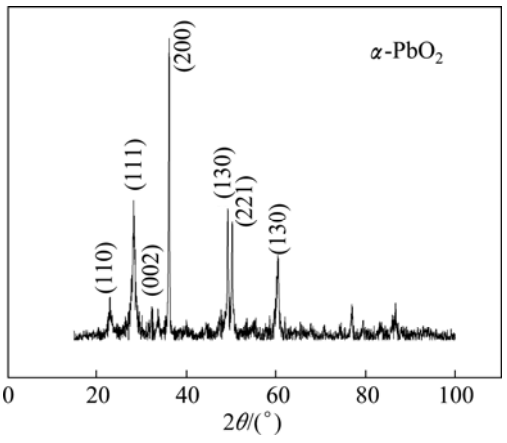

Fig. 1 XRD pattern of α-PbO_2 (scrutinyite)

Table 1 Deposition condition for α-PbO_2 coatings

ρ(NaOH)/(g·L^{-1})	PbO	Current density/(mA·cm^{-2})	pH	Temperature/°C	Plating time/min
180	Saturation	20	9.5−10	40−50	30−40

Table 2 Deposition condition for β-PbO_2 coatings

ρ($Pb(NO_3)_2$)/(g·L^{-1})	ρ($Cu(NO_3)_2$)/(g·L^{-1})	ρ(NaF)/(g·L^{-1})	Current density/(mA·cm^{-2})	pH	Temperature/°C	Plating time/h
190	15	0.5	5	3−3.5	70−80	1

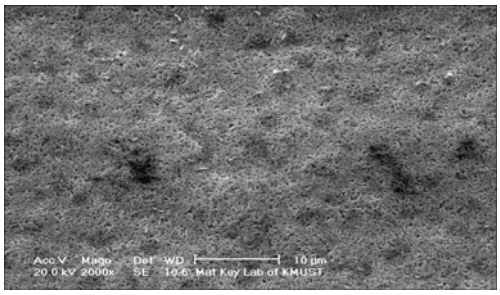

Fig. 2 SEM image of α-PbO_2 coating (scrutinyite)

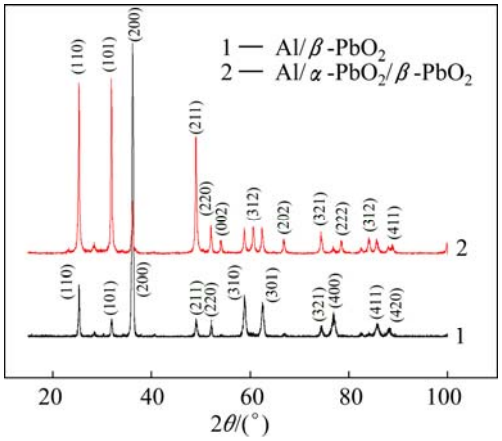

Fig. 3 XRD patterns of β-PbO_2 coatings

No. 2 was prepared on the α-PbO_2 layer. The main crystal plane of No. 1 is (200), while that of No. 2 is (101). The main crystal plane of No. 2 is consistent with the results reported by ABACI et al [26]. Furthermore, No. 2 has more peaks: (002), (312), (202), (222), (312), and they are all consistent with the PDF#41—1492, showing that No. 2 is better crystallized. Apparently, α-PbO_2 as intermediate layer will improve the crystallization of β-PbO_2.

Table 3 shows the ΔG_f^{Θ} values of several substances, which may participate as a reactant or product in producing PbO_2. Table 4 presents the ΔG_r^{Θ} of each reaction and demonstrates that thermodynamic reaction followed by ease of PbO>PbO_2>Pb_2O_3>Pb_3O_4. Figure 4 shows that the precipitation potential of α-PbO_2 is lower than that of β-PbO_2, which requires small electromotive force (E). So, according to the equation: $\Delta G=-nEF$ (ΔG>0), when the product is α-PbO_2, the ΔG is low, the energy barrier is smaller and therefore the thermodynamic stability is poor. Researchers also conducted a study on this issue and came to conclusions that the thermodynamic stability of β-PbO_2 is better than that of α-PbO_2 [29]. Above all, the thermodynamic reaction (precipitation potential) followed by ease of PbO>α-PbO_2>β-PbO_2>Pb_2O_3>Pb_3O_4. In this case, β-PbO_2 coating is more suitable as a surface anode materials.

Table 3 Reactant and product of anodic process and ΔG_f^{Θ} [27,28]

Substance	ΔG_f^{Θ}/(kJ·mol^{-1})
H_2O	−306.39
H^+	6.23
Pb^{2+}	8.11
PbO	−238.43
Pb_2O_3	−531.01
Pb_3O_4	−781.13
PbO_2	−295.59

Table 4 Reaction of anodic process and ΔG_r^{Θ} [27,28]

Reaction	ΔG_r^{Θ}/(kJ·mol^{-1})
$Pb^{2+}+H_2O \rightarrow PbO+2H^+$	72.31
$2Pb^{2+}+3H_2O \rightarrow Pb_2O_3+6H^++2e$	357.98
$3Pb^{2+}+4H_2O \rightarrow Pb_3O_4+8H^++2e$	418.63
$Pb^{2+}+2H_2O \rightarrow PbO_2+4H^++2e$	282.65

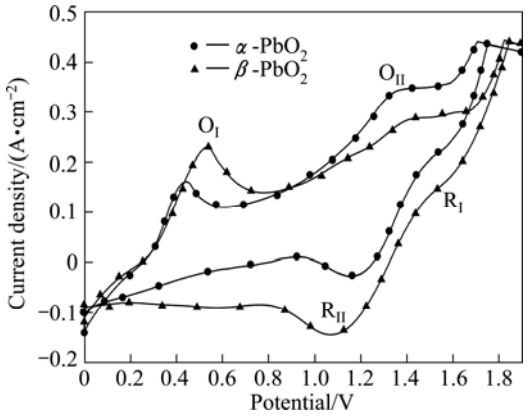

Fig. 4 CV curves of α-PbO_2 and β-PbO_2 coatings (O_I—Oxidation peak I; O_{II}—Oxidation peak II; R_I—Reduction I; R_{II}—Reduction II)

Figure 5(a) presents the β-PbO_2 prepared directly on the conductive layer (β_D), while Fig. 5(b) presents β-PbO_2 prepared on α-PbO_2 layer ($\alpha\beta$). The morphology of the β_D shown in Fig. 5(a) looks like a nappe sheet, whereas that of $\alpha\beta$ looks like a typical pyramid and the average grain size is 25 μm. It is obvious that coatings prepared on the α layer are more compact and uniform. Studies show that [30−32], α-PbO_2 intermediate layer can effectively increase the firmness of the lead dioxide coating and the substrate, and the ease of the distortion of electrodeposition, and make the surface layer β-PbO_2 distribute more uniformly. Therefore, new type of PbO_2 electrode is composed of α-PbO_2 intermediate layer and β-PbO_2 surface layer, so a better catalytic activity is obtained [33].

3.2 CeO_2 as doping agent

The compositional analysis of Al/α-PbO_2/β-PbO_2 electrodeposits was performed under different CeO_2

concentrations in bath using energy dispersive spectroscopy. EDS spectra of β-PbO_2−CeO_2 films deposited under different conditions are shown in Fig. 6. It is found from Fig. 6 that with increasing the CeO_2 concentration in bath from 10 to 50 g/L, Ce contents are 2.97%, 2.90%, 3.47%, 3.44% and 3.73%, respectively.

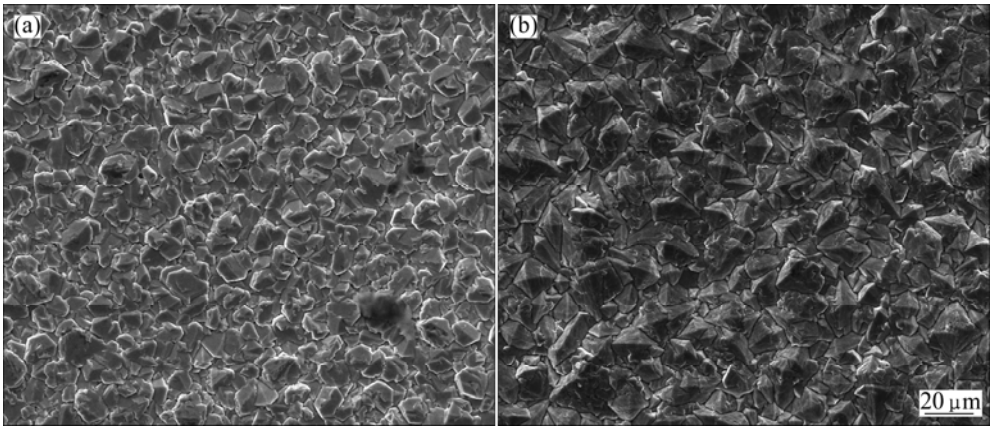

Fig. 5 SEM images of β-PbO_2 prepared directly on conductive layer (a) and on α-PbO_2 layer (b)

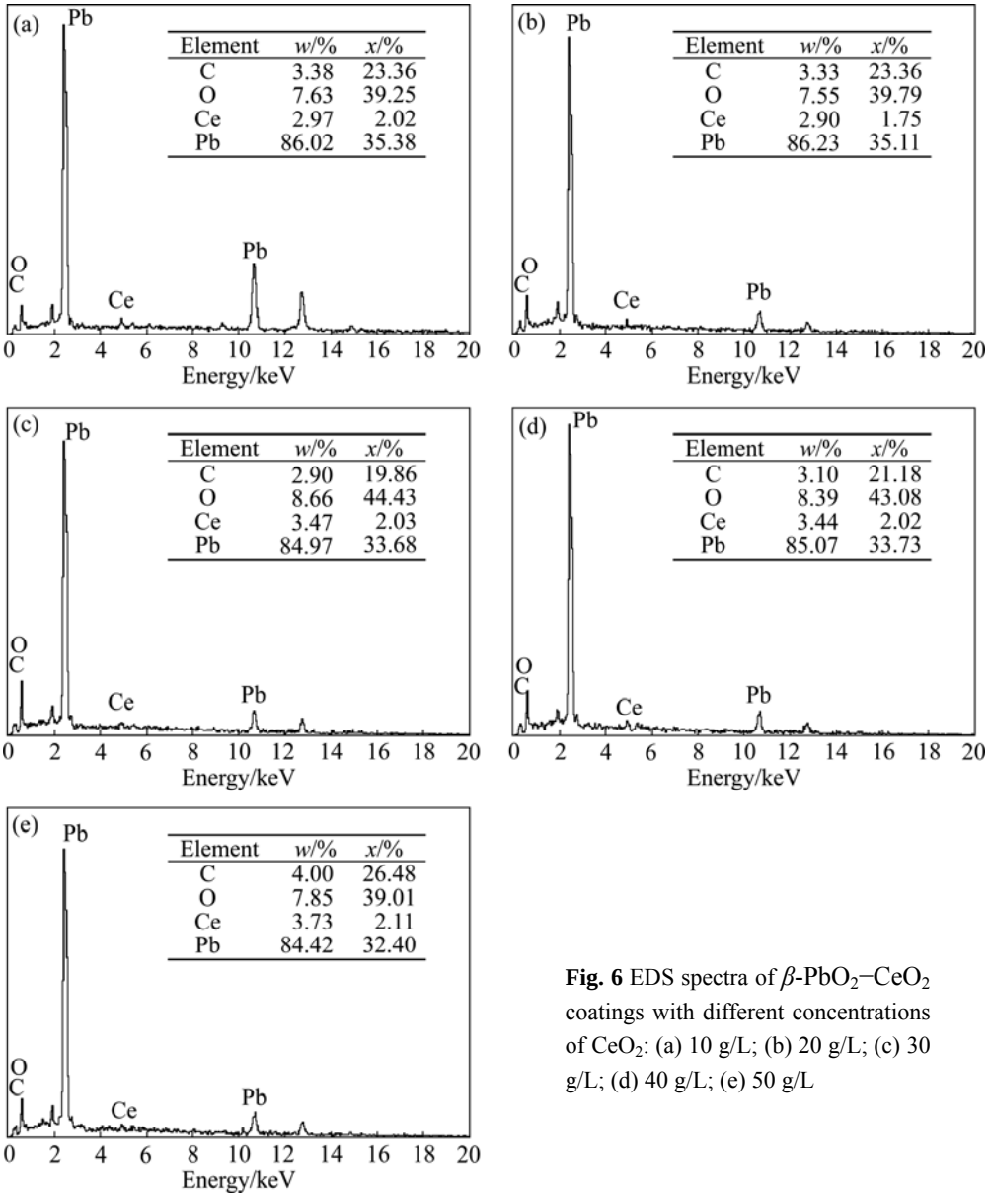

Fig. 6 EDS spectra of β-PbO_2−CeO_2 coatings with different concentrations of CeO_2: (a) 10 g/L; (b) 20 g/L; (c) 30 g/L; (d) 40 g/L; (e) 50 g/L

Obviously, particles will get more opportunity to be embed into Al/α-PbO_2/β-PbO_2 composite by adding more nucleation points on the anodic surface. More particles suspending in the electrolyte are good for CeO_2 to stay, absorb and form nucleation points. As a result, increasing the CeO_2 concentration will surely help the co-deposition. Rare earth oxides can easily catalyze the oxidation of organics and change the surface morphology.

When ceria dioxide is used, as shown in Fig. 7, the surface morphology presents nodular shape. The average grain sizes decrease with the increase of Ce content. The average grain sizes are shown in Table 5. The present experimental results indicate that the crystallization process of PbO_2 can be affected by adulteration of CeO_2, thus changing surface microstructure of the coating. The average grain size of PbO_2 decreases with the adulteration of CeO_2 because the doped ceria dioxide provides a new center for PbO_2 to nucleate, which hinders the further growth of PbO_2. In other words, the nucleation rate is faster than the growing rate [34].

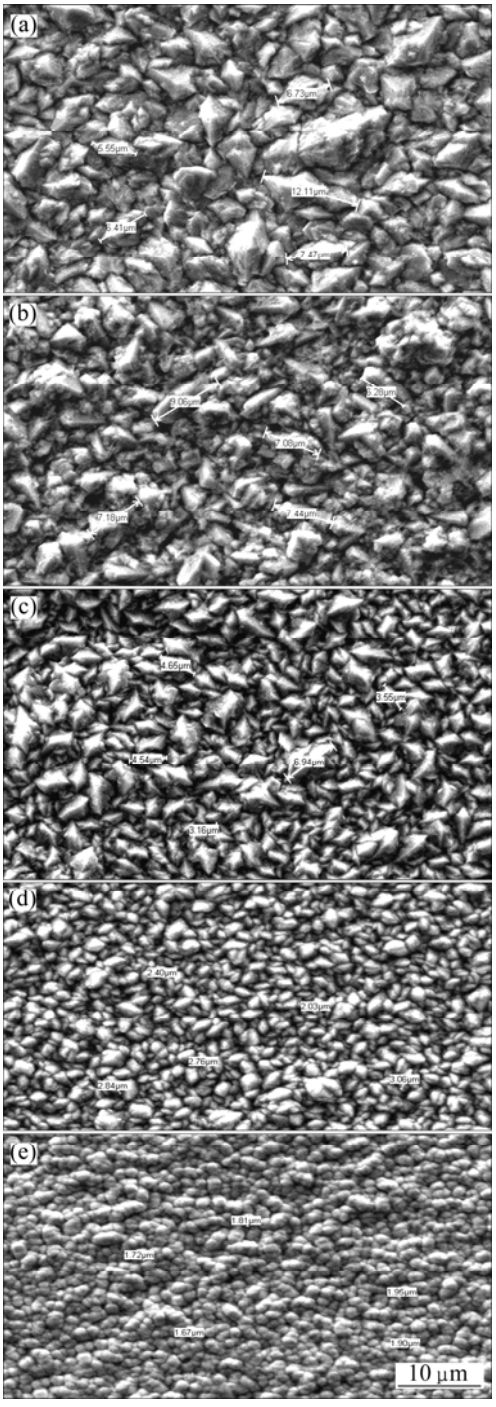

Fig. 7 SEM images of β-PbO_2 with different concentrations of CeO_2: (a) 10 g/L; (b) 20 g/L; (c) 30 g/L; (d) 40 g/L; (e) 50 g/L

Table 5 Grain size of coatings

Sample No.	Minimum size/μm	Maximum size/μm	Average size/μm
1	5.55	12.11	7.67
2	6.28	9.06	7.408
3	3.16	6.94	4.568
4	2.03	3.06	2.618
5	1.67	1.95	1.81

3.3 Over potential and catalytic activity for oxygen evolution

In zinc plating industry, anodic over potential, mainly caused by oxygen evolution reaction, will consume a large percentage of cell voltage. Therefore, a low oxygen evolution potential will save electricity and reduce the cell voltage a lot. Figure 8 gives the polarization curves of Al/α-PbO_2/β-PbO_2−CeO_2 and Al/β-PbO_2 electrodes in 1.3 mol/L $ZnSO_4$+1 mol/L H_2SO_4 (pH=4.5). Compared with Al/α-PbO_2/β-PbO_2, adulteration of CeO_2 can apparently lower the over-potential of PbO_2. According to the Tafel equation:

$$\eta = -\frac{2.3RT}{n\beta F}\lg J^0 + \frac{2.3RT}{n\beta F}\lg J$$

where β is the transfer coefficient and J^0 is the exchange current density, dividing the intercept of linear by its slope, J^0 can be obtained, and the fitting curves are shown in Fig. 9. The exchange current densities are listed in Table 6, confirming that Al/α-PbO_2/β-PbO_2−CeO_2 has a higher catalytic activity for oxygen evolution than Al/β-PbO_2. Moreover, adulteration of CeO_2 can greatly influence the exchange current. When CeO_2 concentration in bath is 30 g/L, the exchange current of Al/α-PbO_2/β-PbO_2−CeO_2 electrode is the highest, indicating that the content of Ce can easily catalyze the oxidation of organics. On the other hand, the surface structure of PbO_2 has a strong influence on the catalytic activity for oxygen evolution [35−37]. The SEM images of Al/α-PbO_2/β-PbO_2−CeO_2 and Al/α-PbO_2/β-PbO_2 electrode show that the morphologies of the two types of electrodes are rather different. The surface of Al/α-PbO_2/

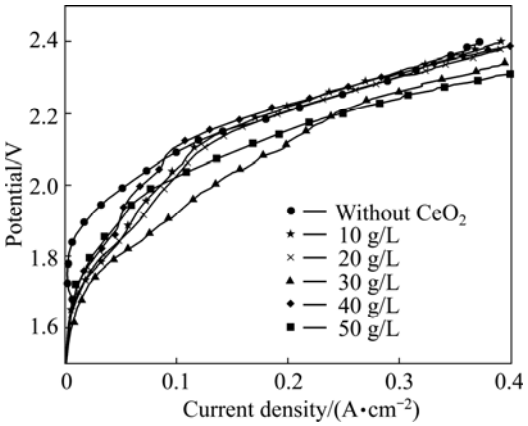

Fig. 8 Polarization curves of PbO_2 electrodes prepared with different concentrations of CeO_2 in bath

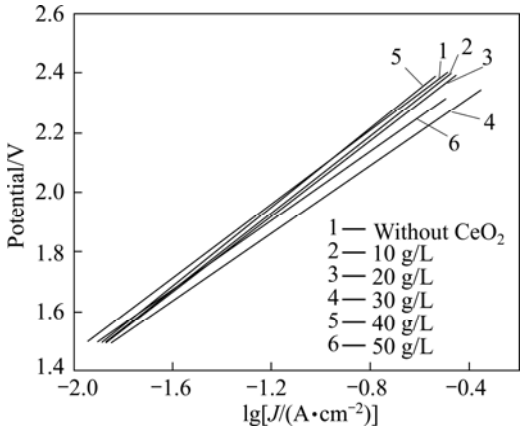

Fig. 9 Linear fitting of polarization curves of PbO_2 electrodes prepared with different concentrations of CeO_2 in bath

Table 6 Kinetic parameters of oxygen evolution

$\rho(CeO_2)/(g\cdot L^{-1})$	a/V	$b/(V\cdot A^{-1})$	$J^0/(A\cdot cm^{-2})$
0	2.535	0.393	3.59×10^{-7}
10	2.599	0.518	9.73×10^{-6}
20	2.562	0.515	5.99×10^{-6}
30	2.637	0.467	1.07×10^{-5}
40	2.522	0.486	5.46×10^{-6}
50	2.529	0.450	5.89×10^{-6}

a: Slope; b: Intercept; J^0: Exchange current density.

β-PbO_2 electrode presents many micro-cracks, and looks like a typical pyramid shape; the grains are more dispersive and large. Al/α-PbO_2/β-PbO_2-CeO_2 is quite compact, and the grain size decreases. Therefore, the active surface area of Al/α-PbO_2/β-PbO_2−CeO_2 electrode is larger than that of Al/β-PbO_2. Moreover, electronic conduction exists in the rare earth oxides [38]. This demonstrates that ceria dioxide, as the catalytic sites, could strengthen the interface electron transfer of the electrode.

3.4 AC impedance

Figure 10 shows the Nyquist plots of the coatings prepared under different CeO_2 concentrations. It can be seen that when CeO_2 concentrations are 10 and 50 g/L, the plots are not the same as the others. Apparently, CeO_2 as a doping agent changes the reaction mechanism. Coatings, which were prepared under CeO_2 concentrations of 10 and 50 g/L, are coarse or can easily fall off. Therefore, only the other three were computed and analyzed. When CeO_2 concentration is 20−40 g/L, polarization resistance (R_p) becomes large first and then gets small. When the fitting software (ZSimpWin) is used to fit and interpret the Nyquist plots, the obtained equivalent circuit is shown in Fig. 11 and the impedance fitting values are listed in Table 7. The equivalent circuit is composed of a solution resistance (R_s), two constant phase elements Q (CPE) which represent the coating capacitance and the double layer capacitance, a coating resistance and a charge transfer resistance (R_{ct}). Generally, CPE/Q may exist because of the rough surface or uneven distribution of the electric field [39]. Table 7 shows that the values of n_1 are all equal to 1, indicating that dispersion effect does not occur between the solution/coating layers. While values of n_2 are all not equal to 1, indicating that dispersion effect occurs under the coating layer, or maybe occurs in electric double layer. When the value of n_2 is closer to 1, the coating layer is smoother and dispersion effect is weaker. When

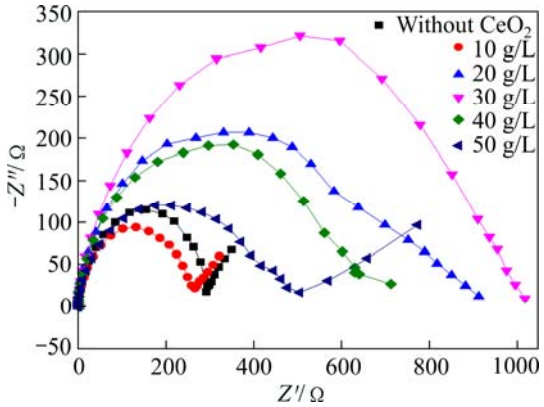

Fig. 10 Nyquist plots of coatings with different CeO_2 concentrations

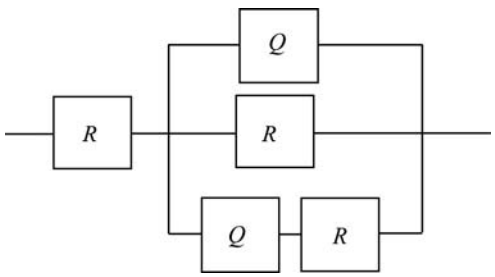

Fig. 11 Equivalent circuit of composite coatings in zinc plating solution

Table 7 Fitting parameters of equivalent circuit of electrode

$\rho(CeO_2)/(g\cdot L^{-1})$	$R_s/(\Omega\cdot m^{-2})$	Q_1(CPE)/(μF·m^{-2})	n_1	$R_d/(\Omega\cdot m^{-2})$	Q_2 (CPE)/(μF·m^{-2})	n_2	$R_{ct}/(\Omega\cdot m^{-2})$
20	0.6648	1.183×10^{-5}	1	840.1	8.571×10^{-5}	0.6447	605.4
30	0.6321	8.409×10^{-6}	1	998.9	4.03×10^{-5}	0.6957	686.1
40	0.6402	1.363×10^{-5}	1	302.4	6.11×10^{-4}	0.4641	447.5

CeO_2 concentration is 30 g/L, dispersion effect of the coating is weaker in that n_2 is maximum, which demonstrates a smoother surface. It is considered that in the low-frequency area, the corrosion resistance of the composite coatings can be reflected by the impedance. Such impedance corresponds to the the charge transfer resistance (R_{ct}). R_{ct} of the three coatings is not very different, only about 100 Ω/cm^2. As the same as the dispersion effect, the largest R_{ct} is tested on the coating when CeO_2 concentration is 30 g/L. This is probably because CeO_2 particles are firstly absorbed on the coating surface, by lowing the reaction area, formation of the oxidation and hydrated layer was hindered, and therefore R_{ct} increases. When CeO_2 particles are wrapped into the metal composite, the reaction area or active area is exposed again, oxidation and hydration occur, and then R_{ct} decreases. This is probable why coatings will have different mechanisms when prepared with different CeO_2 concentrations. Particles experience a complex process, including adsorption→desorption→inlay→coating. So the composite deposition process is actually complicated.

4 Conclusions

1) α-PbO_2 as intermediate layer can improve the deposition of β-PbO_2, including structure and crystal plane. β-PbO_2 has better thermodynamic stability, and is more suitable as a surface layer.

2) Rare earth oxide dopants can decrease the grain size of PbO_2 and enlarge the active surface area and therefore change the content of Ce element in the coating.

3) The change of catalytic activity is mainly due to the specific role of the doped ceria dioxide and the different structures of electrodes.

References

[1] ZHI G Y, HUI M M, DONG B S. New degradation mechanism of Ti/IrO_2+MnO_2 anode for oxygen evolution in 0.5 M H_2SO_4 solution [J]. Electrochimica Acta, 2008, 53(18): 5639−5643.

[2] PANICA V V, JOVANOVICA V M, TERZICA S I , BARSOUMB M W, JOVICC V D, DEKANSKIA A B. The properties of electroactive ruthenium oxide coatings supported by titanium-based ternary carbides [J]. Surface and Coatings Technology, 2007, 202: 319−324.

[3] AROMAA J, FORSEN O. Evaluation of the electrochemical activity of a Ti−RuO_2−TiO_2 permanent anode [J]. Electrochimica Acta, 2006, 51(27): 6104−6110.

[4] ZHAO Q, LIU Y, MULLER-STEINHAGEN H, LIU G. Graded Ni−P−PTFE coatings and their potential applications [J]. Surface and Coatings Technology, 2002,155: 279−284.

[5] FENG Q Y, LI T J, JIN J Z. Research on the mechanism of composite electroplating and its latest progress rare metal materials and engineering [J]. Rare Metal Materials and Engineering, 2007, 36(3): 559−564. (in Chinese)

[6] BIRAME B, ENRIC B, BEATRICE M, PIERRE ALAIN M, CHRISTOS C, GIUSEPPE F, GIANCARL S. Electrochemical incineration of chloromethylphenoxy herbicides in acid medium by anodic oxidation with boron-doped diamond electrode [J]. Electrochim Acta, 2006, 51(15): 2872−2880.

[7] CARLOS A M H, MARCO A Q, CHRISTOS C, SERGIO F, ACHILLE D B. Electrochemical incineration of chloranilic acid using Ti/IrO_2, Pb/PbO_2 and Si/BDD electrodes [J]. Electrochim Acta, 2004, 50(4): 949−956.

[8] CARMEM L P S Z, PIERRE-ALAN M, CHRISTOS C, ADALGISA R, DE A, JULIEN F C B. Electrochemical oxidation of p-chlorophenol on SnO_2–Sb_2O_5 based anodes for wastewater treatment [J]. Journal of Applied Electrochemistry, 2003, 33(12): 1211−1215.

[9] PANIC V V, DEKANSKI A B, VIDAKOVIC T R, MISKOVIC-STANKOVIC V B, JAVANOOVIC B Z, NIKOLIC V Z. Oxidation of phenol on RuO_2–TiO_2/Ti anodes [J]. Solid State Electrochem, 2005, 9(1): 43−54.

[10] WANG Y H, CHENG S, CHAN K Y, LI X Y. Electrolytic generation of ozone on antimony- and nickel-doped tin oxide electrode [J]. Journal of The Electrochemical Society, 2005, 152(11): D197−D200.

[11] CARR J P, HAMPSON N A. The lead dioxide electrode [J]. Chemical Reviews, 1972, 72(6): 679−702.

[12] PETERSSON I, AHLBERG E, BERGHULT B. Parameters influencing the ratio between electrochemically formed α and β-PbO_2 [J]. Journal of Power Sources, 1998, 76(1): 98−105.

[13] AMADELLI R, MALDOTTI A, MOLINARI A, DANILOV F I, VELICHENKO A B. Influence of the electrode history and effects of the electrolyte composition and temperature on O_2 evolution at β-PbO_2 anodes in acid media [J]. Journal of Electroanalytical Chemistry, 2002, 534(1): 1−12.

[14] PAVLOV D, MONAHOV B. Mechanism of the elementary electrochemical processes taking place during oxygen evolution on the lead dioxide electrode [J]. Journal of The Electrochemical Society, 1996, 143(11): 3616−3629.

[15] MUNICHANDRAIA N, SATHYANARAYANA S. Insoluble anode of α-lead dioxide coated on titanium for electrosynthesis of sodium perchlorate [J]. Journal of Applied Electrochemistry, 1988, 18(2): 314−316.

[16] ABACI S, PEKMEZ K, PEKMEZ P, YILDIZ A. Electrocatalysis of polyaniline formation by PbO_2 in acetonitrile [J]. Journal of Applied Polymer Science, 2003, 87(4): 599−605.

[17] ABACI S, TAMER U, PEKMEZ K, YILDIZ A. Electrosynthesis of 4,4′-dinitroazobenzene on PbO_2 electrodes [J]. Journal of Applied

Electrochemistry, 2002, 32(2): 193−196.
[18] ABACI S, YILDIZ A. Electropolymerization of thiophene and 3-methylthiophene on PbO_2 electrodes [J]. Journal of Electroanalytical Chemistry, 2004, 569(1): 161−168.
[19] VELICHENKO A B, AMADELLI R, BENEDETTI A, GIRENKO D V, KOVALYOV S V, DANILOVA F I. Electrosynthesis and physicochemical properties of PbO_2 films [J]. Journal of The Electrochemical Society, 2002, 149(9): C445−C449.
[20] UEDA M, WATANABE A, KAMEYAMA T, MATSUMOTO Y, SEKIMOTO M, SHIMAMUNE T. Performance characteristics of a new type of lead dioxide-coated titanium anode [J]. Journal of Applied Electrochemistry, 1995, 25: 817−822.
[21] CATTARIN S, GUERRIERO P, MUSIANI M. Preparation of anodes for oxygen evolution by electrodeposition of composite Pb and Co oxides [J]. Electrochim Acta, 2001, 46(26−27): 4229−4234.
[22] CATTARIN S, FRATEUR I, GUERRIERO P, MUSIANI M. Electrodeposition of PbO_2+CoO_x composites by simultaneous oxidation of Pb^{2+} and Co^{2+} and their use as anodes for O_2 evolution [J]. Electrochim Acta, 2000, 45: 2279−2288.
[23] MUSIANI M, GUERRIERO P. Oxygen evolution reaction at composite anodes containing Co_3O_4 particles [J]. Electrochim Acta, 1998, 44(8−9): 1499−1507.
[24] MUSIANI M, FURLANETTO F, GUERRIEROP. Electrochemical deposition and properties of PbO_2+Co_3O_4 composites [J]. Journal of Electroanalytical Chemistry, 1997, 440(1−2): 131−138.
[25] SRIVASTAVA M, WILLIAM GRIPS V K, RAJAM K S. Electrodeposition of Ni−Co composites containing nano-CeO_2 and their structure, properties [J]. Applied Surface Science, 2010, 257(3): 717−722.
[26] ABACI S, PEKMEZ K, HOKELEK T, YILDIZ A. Investigation of some parameters influencing electrocrystallisation of PbO_2 [J]. Journal of Power Sources, 2000, 88(2): 232−236.
[27] LI Di. Electrochemical principle [M]. Beijing: Beihang University Press, 1999. (in Chinese)
[28] LI Wen-chao. Metallurgical and materials physical chemistry [M]. Beijing: Metallurgical Industry Press, 2001. (in Chinese)
[29] ZHOU Ya-ning, WAN Ya-zhen, LIU Jin-dun. Preparation and application of PbO_2 electrode [J]. Salt Industry, 2006, 38(10): 8−11. (in Chinese)
[30] WENG Feng, YU Bin. Preliminary research of determining COD using Pt/PbO_2 electrode [J]. Journal of Nanjing University of Technology, 2002, 24(2): 93−96.
[31] PETERSSON I, AHLBERG E, BERGHULT B. Parameters influencing the ratio between electro-chemically formed α and β-PbO_2 [J]. Journal of Power Sources, 1988, 76(1): 98−105.
[32] FUKASAWA A. Production of commercial large lead dioxide electrode-application of a new-type lead dioxide electrode to electrolytic refining [J]. Mining and Metallurgical Institute of Japan, 1984, 1157: 599−602.
[33] ZHANG Zhao-xian. Titanium electrode industry [M]. Beijing: Metallurgical Industry Press, 2000. (in Chinese)
[34] CASELLATO U, CATTARIN S, MUSIANI M. Preparation of porous PbO_2 electrodes by electrochemical deposition of composites [J]. Electrochim Acta, 2003, 48(27): 3991−3998.
[35] AMADELLI R, ARMELAO L, VELICHENKO A B, NIKOLENKO N V, GIRENKO D V, KOVALYOV S V, DANILOV F I. Oxygen and ozone evolution at fluoride modified lead dioxide electrodes [J]. Electrochim Acta, 1999, 45: 713−720.
[36] ABACI S, PEKMEZ K, HOKELEK, YILDIZ A. Investigation of some parameters influencing electrocrystallisation of PbO_2 [J]. Journal of Power Sources, 2000, 88(2): 232−236.
[37] HO J C K, TREMILIOSI G, SIMPRAGA R, CONWAY B E, Structure influence on electrocatalysis and adsorption of intermediates in the anodic O_2 evolution at dimorphic alpha-PbO_2 and beta-PbO_2 [J]. Journal of Electroanalytical Chemistry, 1994, 366(5):147−162.
[38] MINACHEV F M. The application of rare earth for catalyst [M]. Beijing: Science Press, 1987. (in Chinese)
[39] LU Chang-feng, LU Min-xu, ZHAO Guo-xian, BAI Zhen-quan, YAN Mi-lin, YANG Yan-qing. The analysis of electrode reactions of CO_2 corrosion of N80 steel [J]. Acta Metallurgica Sinica, 2002, 38(7): 770−774. (in Chinese)

纳米 CeO_2 对电沉积 Al/α-PbO_2/β-PbO_2 镀层结构和性能的影响

陈 阵[1]，余 强[1]，廖登辉[2]，郭忠诚[2]，武 剑[2]

1. 昆明理工大学 理学院，昆明 650093；
2. 昆明理工大学 冶金与能源工程学院，昆明 650093

摘 要：采用阳极氧化法制备掺杂稀土氧化物(CeO_2)的 Al/α-PbO_2/β-PbO_2 复合电极，考察 CeO_2 的掺杂以及 α-PbO_2 作为中间层对 Al/α-PbO_2/β-PbO_2 电极性能的影响。结果表明：α-PbO_2 作为中间层有利于 β-PbO_2 的结晶，β-PbO_2 比 α-PbO_2 更适合作电极表层；CeO_2 的掺杂能够改变晶粒尺寸和晶粒结构，提高电极的催化活性，并改变 PbO_2 晶粒的沉积机理；掺杂 CeO_2 的 PbO_2 电极的电催化活性能得到有效提高，从而降低析氧电位和槽电压。

关键词：稀土；CeO_2；复合电极材料；α-PbO_2；β-PbO_2；槽电压；惰性阳极

(Edited by Xiang-qun LI)